Highly Effective Wound Healing Enabled by Discrete Alternative Electric Fields from A Wearable Nanogenerator

Yin Long, [1,3†]Hao Wei,[2,4†] Jun Li,[1] Guang Yao,[1,3] Bo Yu, [2] Dalong Ni,[2] Angela LF Gibson,[5] Xiaoli Lan,[4] Yadong Jiang,[3] Weibo Cai[2,*] and Xudong Wang,[1,*]

1. Department of Materials Science and Engineering, University of Wisconsin-Madison, Madison, Wisconsin 53706, United States
2. Department of Radiology and Medical Physics, University of Wisconsin-Madison, Madison, Wisconsin 53705, United States
3. State Key Laboratory of Electronic Thin Films and Integrated Devices, University of Electronic Science and Technology of China, Chengdu, 610054, China
4. Department of Nuclear Medicin, Union Hospital, Tongji Medical College, Huazhong University of Science and Technology, Wuhan, 430073, China
5.Department of Surgery, University of Wisconsin-Madison, Madison, Wisconsin 53792, United States

*Email: xudong.wang@wisc.edu (XW) and wcai4@wisc.edu (WC)

S1.

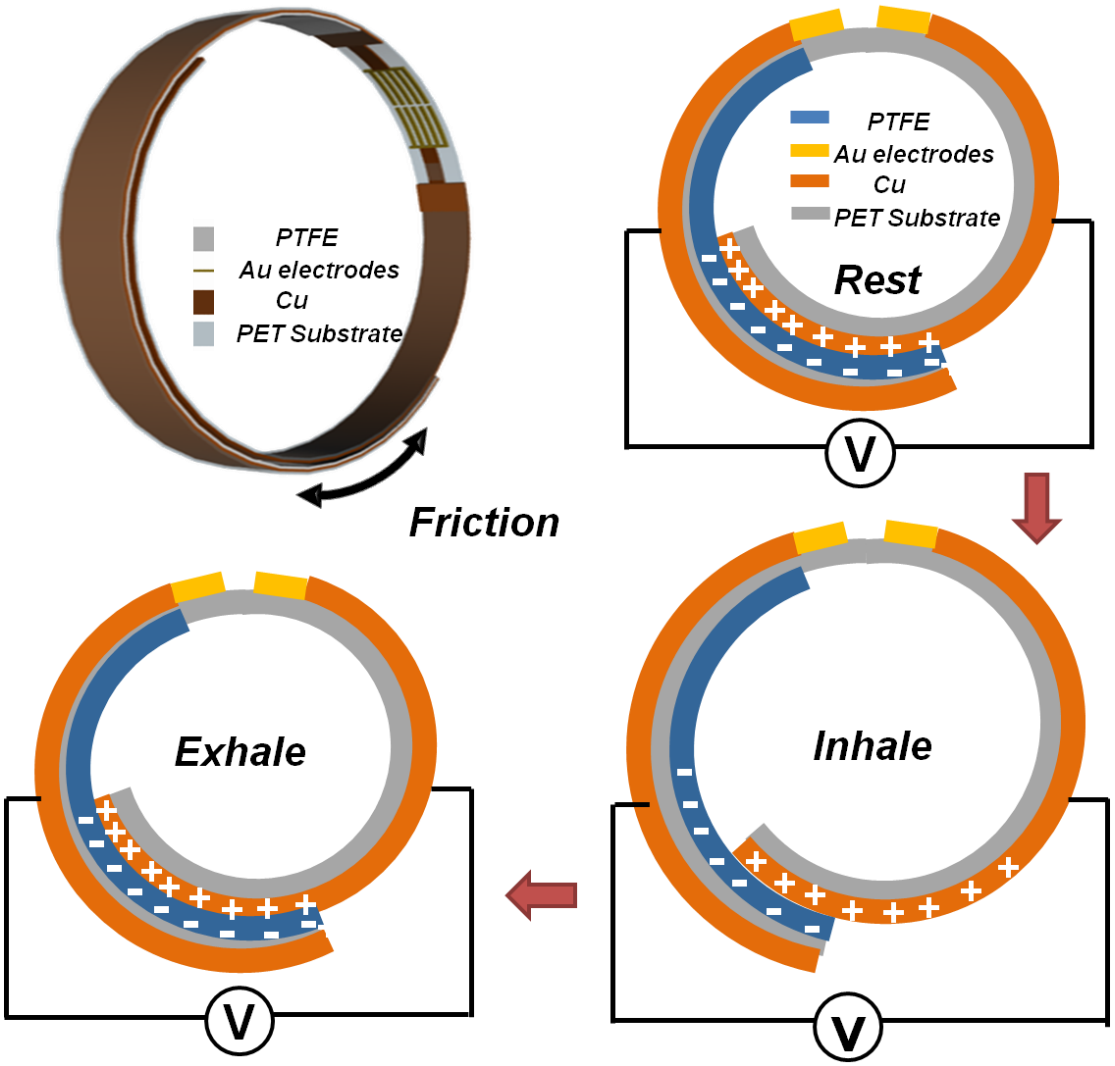

Figure S1. Schematic of electricity generated by bandage using rat's breathing pattern.

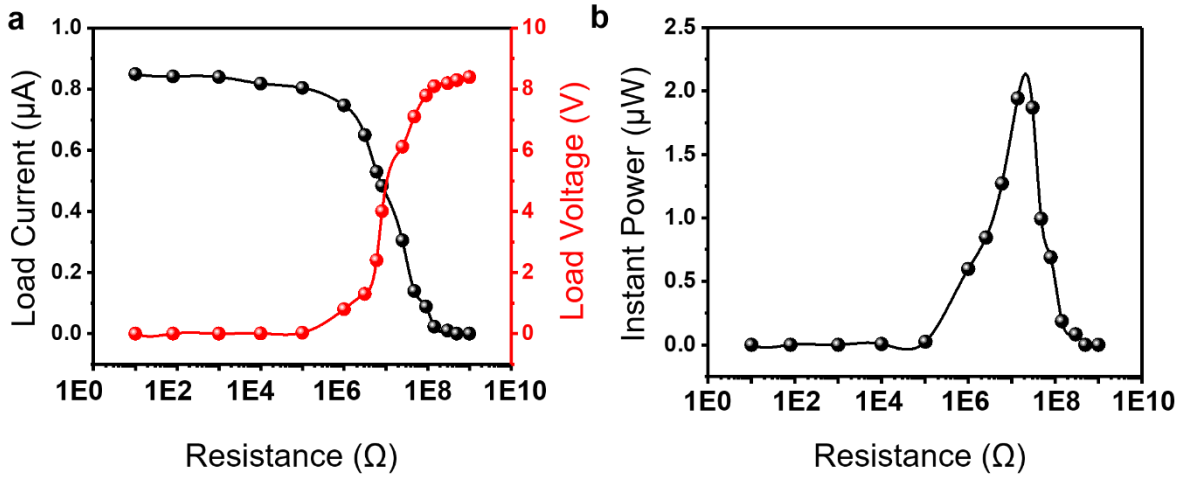

Figure S2. **a.** The voltage and current and **b.** calculated power outputs as a function of load resistances.

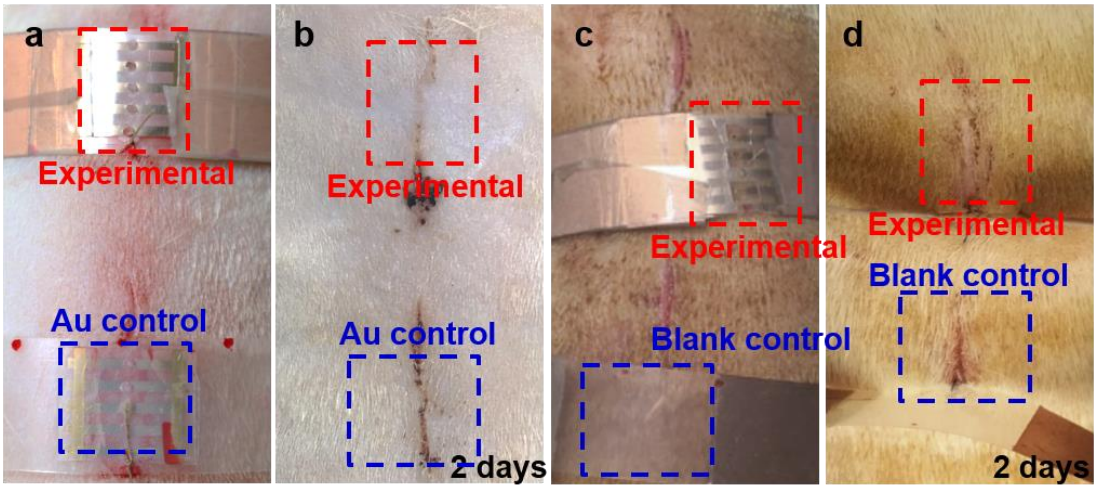

Figure S3. Healing of linear wounds treated with perpendicular alignment of electrode pairs. **a.** Photograph of day 0 experimental and Au control groups. **b.** Photograph of day 2 experimental and Au control groups. **c.** Photograph of day 0 experimental and blank control groups. **d.** Photograph of day 2 experimental and blank control groups.

Figure S4. Photograph of electrodes tie closely to rat's skin after 7 days.

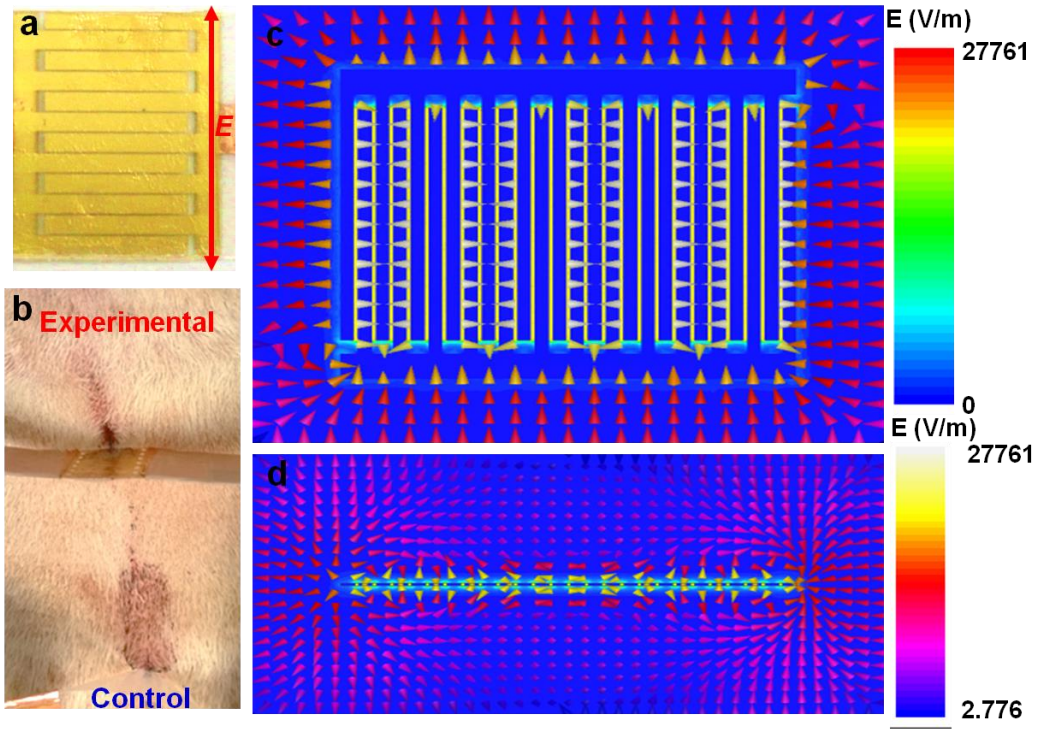

Figure S5. Small wound's healing experiment under interdigitated electrodes. **a.** Digital image of interdigitated electrodes. **b.** 2 days' healing under interdigitated electrodes configuration (experimental) and blank control. **c.** Front and **d.** Lateral view of electric simulation of the interdigitated electrodes

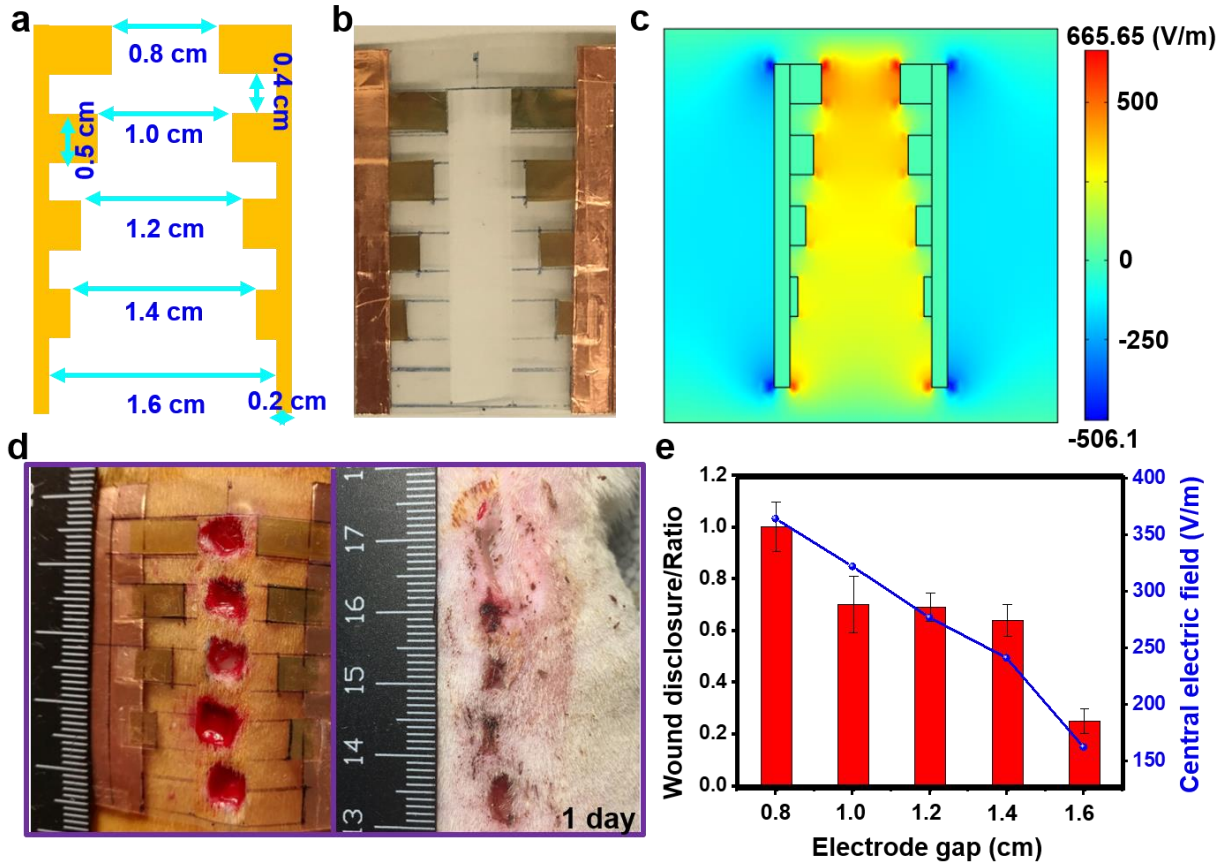

Figure S6. **a.** Schematic, **b.** real demonstration and **c.** electric field simulation of the finger electrodes. **d.** Photograph of distributed wounds healed under distributed electrodes. **e.** Ratio of wound disclosure under different electrode gaps after 1-day treatment (n=4).

To understand the electric field strength influences on would healing, a parallel electrode set was designed and tested on square wounds. Figure S6a and b show the new electrode pattern. It had five pairs of electrodes with their electrode gaps varied from 0.8 cm to 2.2 cm to applied different electric field strength simultaneous. The simulation results (Figure S6c) showed that the electric field distribution in between these electrodes, and the intensity decreased when the electrode gap increasing. Five full thickness wounds (around 0.4 cm × 0.4 cm) were created along the dorsal of each rat, and treated under distributed electrodes (Figure S6d). The ratio of wound disclosure were recorded and the results were shown in Figure S6e. The corresponding average electric field strengths between each pair of electrode were extracted from the simulation and plotted together

in Figure S6e. The 0.8 cm gap electrodes showed a full re-epithelization and the therapeutic effects became less significant as the electrode gap increased. The 1.6 cm gap electrode pair showed the lowest wound disclosure.

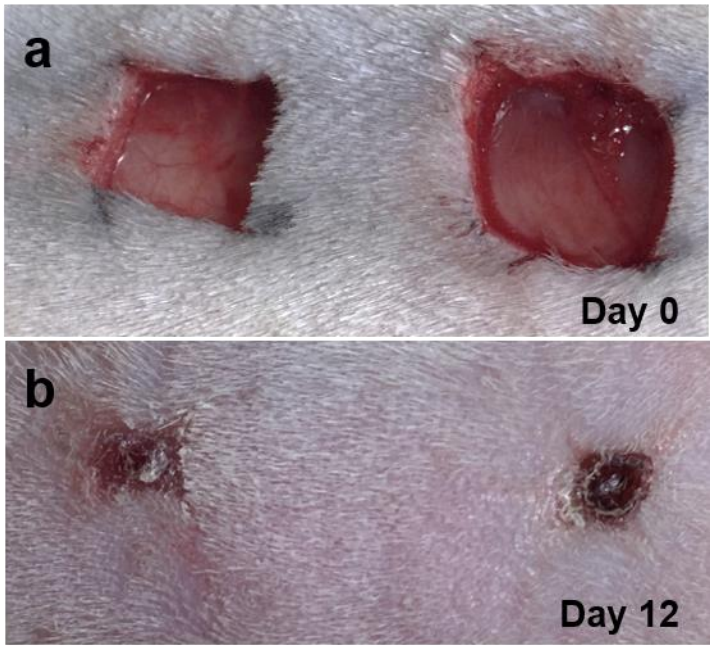

Figure S7. a. Full thickness wounds of 0.8 cm × 0.8 cm at day 0. **b.** Naturally healed wounds due to contraction after 12 days.

For natural wounds healing process, wounds (Figure S7a) will create a low resistance pathway through which current will flow. This current flow from regions around the wound will generates a lateral electric filed pointing toward the center of wound. The range of this naturally presented field is called endogenous electric field, and its strength is ranged from ~40 to 200 mV/mm. The skin cells move along this electric field, resulting in natural wounds heals towards the center, as shown in Figure S6b.

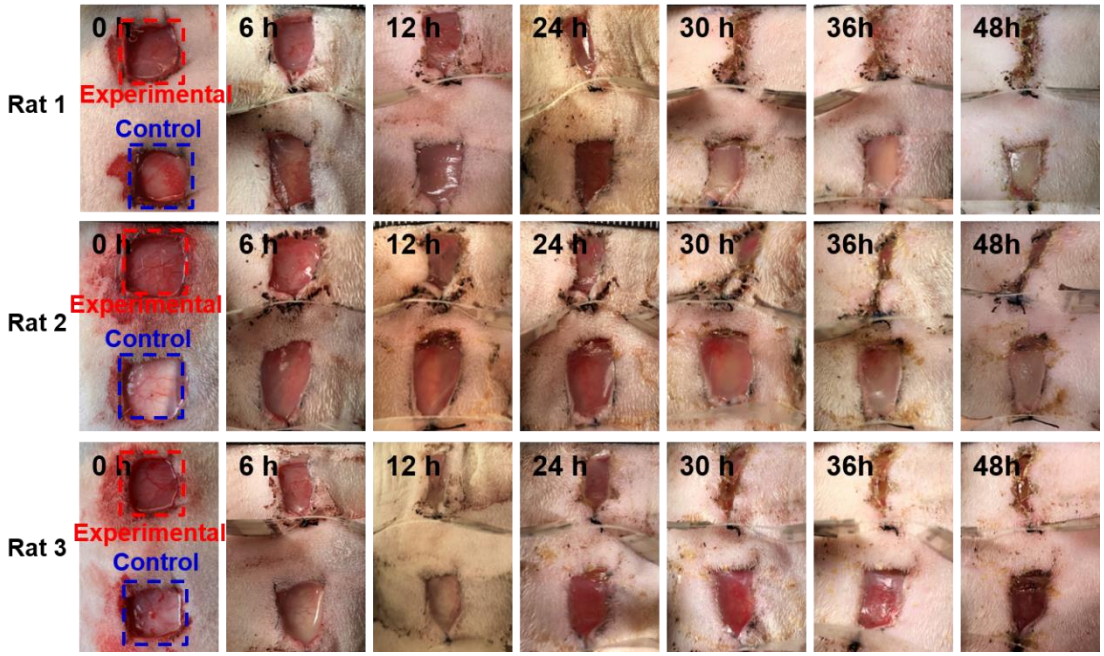

Figure S8. Serial photographs of scaled wounds (0.8 cm ×0.8 cm) in 3 rats. Top: Nanogenerator; Bottom: Control.

When the electric field from a NG is applied, the healing rate along the direction of NG electric field was much accelerated, as shown in Figure 3c and Figure S6. This revealed that the NG electric field predominated the healing effects and the wound quickly contracted and re-epithelialized along the external field direction. In the control group, we can still find wounds contracted and heal toward the center following the natural direction. However, by comparing the length of the wounds, we can see that NG-dressed wounds remained a nearly constant length perpendicular to the electric field direction; while the wound was nearly closed along the electric field direction. The control showed an obviously reduced length along the same direction. This fact shows that the natural healing behavior might be suppressed, because if the natural process still played, reduced wound length should be observed from the NG-dressed wounds.

This phenomenon can be understood based on the principle of endogenous electric field. When a strong external electric field is applied, the current flow direction will be tuned – enhanced along the parallel direction, but suppressed along the perpendicular direction. This common electric behavior could diminish the endogenous electric field along the perpendicular direction, and thus suppress the natural healing process.

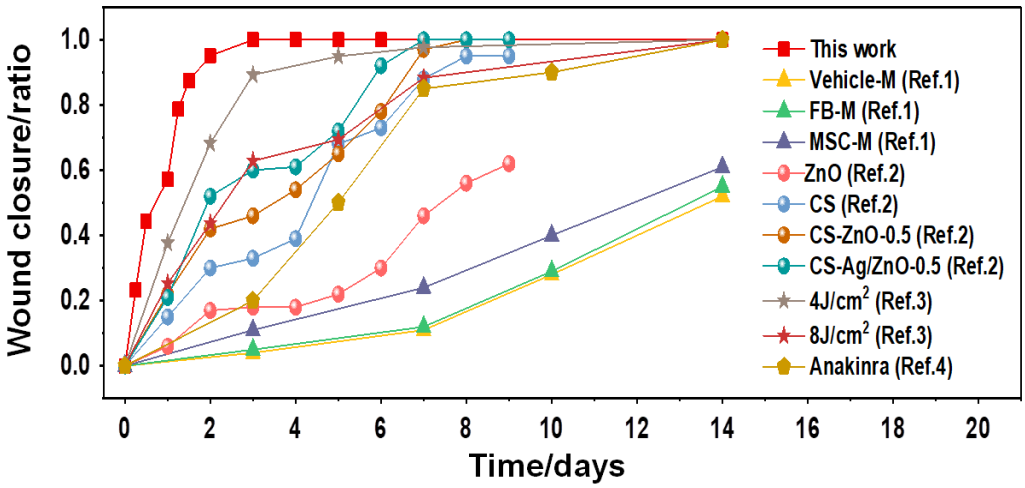

Figure S9. Comparison of would closure as a function of time under the stimulations of different techniques.[1-4]

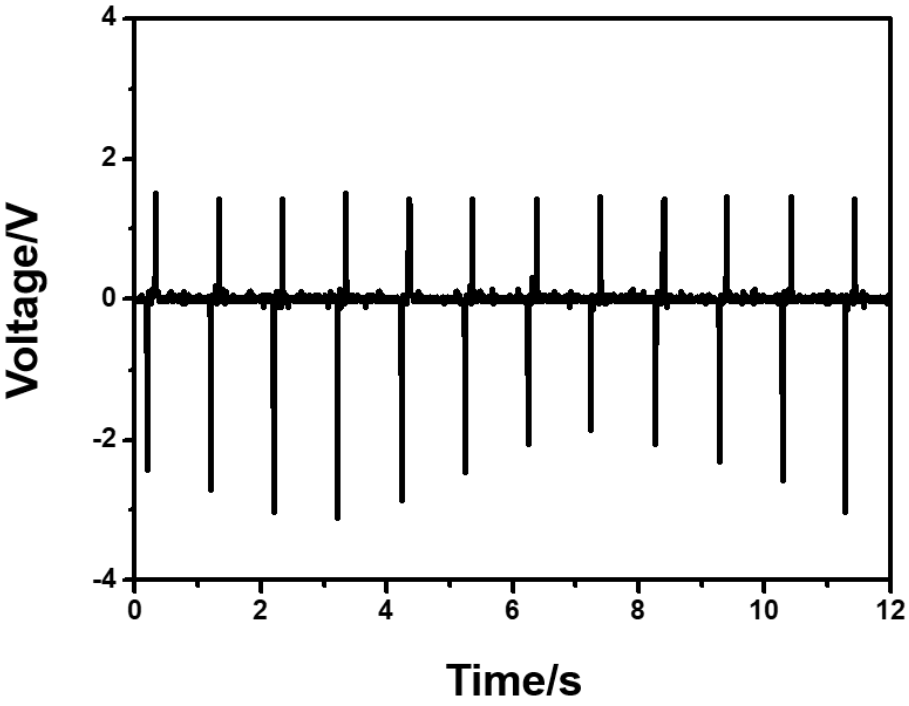

Figure S10. Voltage outputs of contact-mode NG

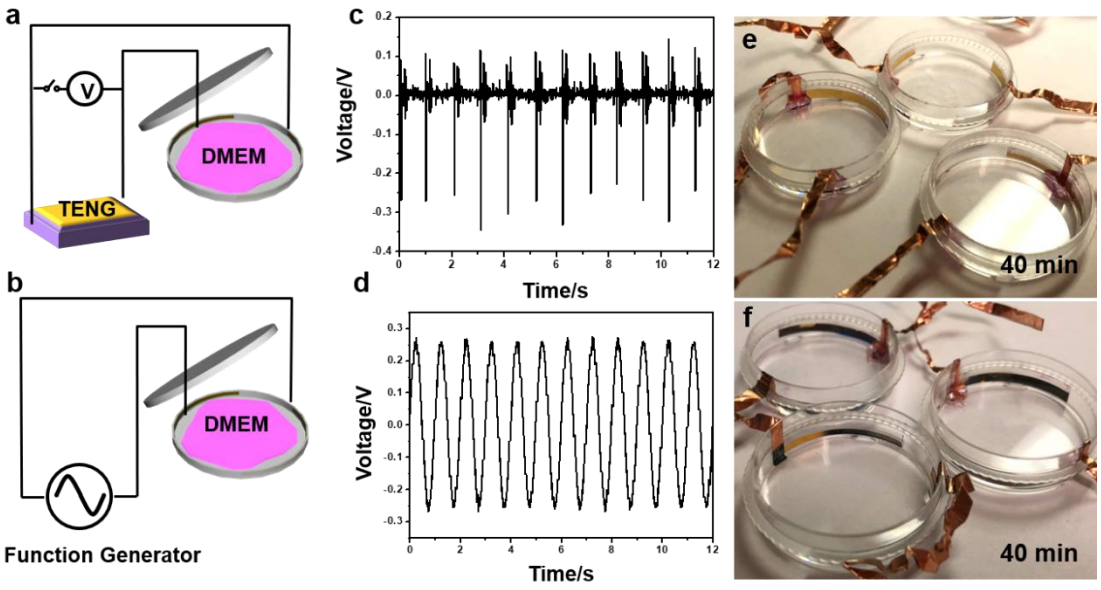

Figure S11. ROS test experiment of blank control, alternating potential generated by **a.** NG and **b.** Function generator. **c.** Voltage output of NG and **d.** Function generator. **e.** Digital image of electrodes morphology after 40 min under NG and **f.** Function generator

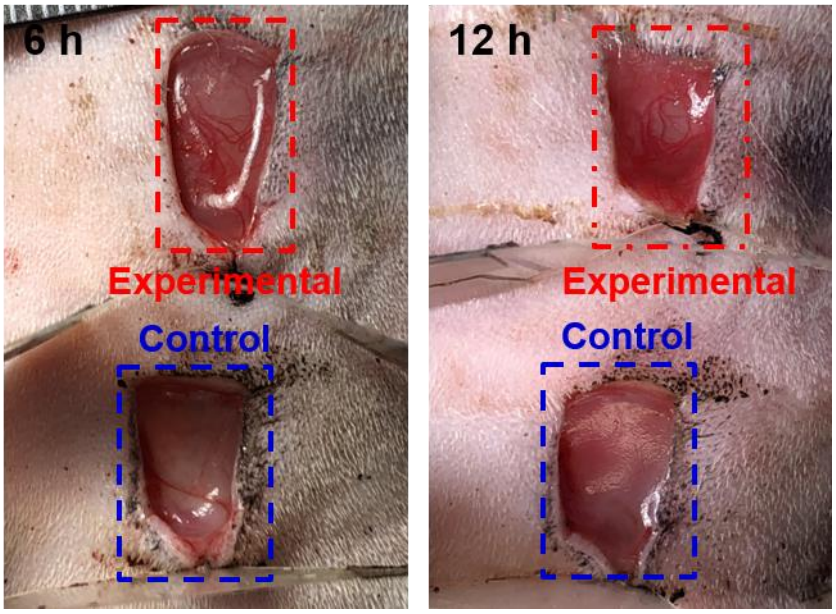

Figure S12. Digital images of blood vessel proliferation in wound area with (experimental group) and without (control group) electric field.

Reference

1. Chen, L.; Tredget, E. E.; Wu, P. Y.; Wu, Y., Paracrine Factors of Mesenchymal Stem Cells Recruit Macrophages and Endothelial Lineage Cells and Enhance Wound Healing. *PLoS One* **2008,** *3*, e1886.

2. Lu, Z.; Gao, J.; He, Q.; Wu, J.; Liang, D.; Yang, H.; Chen, R., Enhanced Antibacterial and Wound Healing Activities of Microporous Chitosan-Ag/Zno Composite Dressing. *Carbohydr. Polym.* **2017,** *156*, 460-469.

3. Medrado, A. R.; Pugliese, L. S.; Reis, S. R. A.; Andrade, Z. A., Influence of Low Level Laser Therapy on Wound Healing and Its Biological Action Upon Myofibroblasts. *Lasers Surg. Med.* **2003,** *32*, 239-244.

4. Kou, X.; Xu, X.; Chen, C.; Sanmillan, M. L.; Cai, T.; Zhou, Y.; Giraudo, C.; Le, A.; Shi, S., The Fas/Fap-1/Cav-1 Complex Regulates Il-1ra Secretion in Mesenchymal Stem Cells to Accelerate Wound Healing. *Sci. Transl. Med.* **2018,** *10*, eaai8524.